ACS APPLIED MATERIALS & INTERFACES

Energy, Environmental, and Catalysis Applications

Immobilization of a Polar Sulfone Moiety onto the Pore Surface of a Humid Stable MOF for Highly Efficient CO2 Separation under Dry and Wet Environment through Direct CO2-Sulfone Interactions

ARUN PAL, Santanu Chand, David Gerard Madden, Douglas M. Franz, Logan Ritter, Brian Space, Teresa Curtin, Shyam Chand Pal, and Madhab C. Das

ACS Appl. Mater. Interfaces, **Just Accepted Manuscript** • DOI: 10.1021/acsami.0c07380 • Publication Date (Web): 17 Aug 2020

Immobilization of a Polar Sulfone Moiety onto the Pore Surface of a Humid Stable MOF for Highly Efficient CO_2 Separation under Dry and Wet Environment through Direct CO_2-Sulfone Interactions

Arun Pal[a], Santanu Chand[a], David G. Madden[b], Douglas Franz[c], Logan Ritter[c], Brian Space[c], Teresa Curtin[d], Shyam Chand Pal[a] and Madhab C. Das*[a]

[a]*Department of Chemistry, Indian Institute of Technology Kharagpur, Kharagpur-721302, India*

[b]*Department of Chemical Engineering & Biotechnology, University of Cambridge, Philippa Fawcett Dr, Cambridge, CB3 0AS, UK*

[c]*Department of Chemistry, University of South Florida, 4202 E. Fowler Ave., CHE205 Tampa, FL 33620-5250*

[d]*Bernal Institute and Department of Chemical Sciences, University of Limerick, Limerick V94 T9PX, Ireland*

KEYWORDS: breakthrough selectivity, CO_2 capture and separations, GCMC calculation, humid stable MOF, IAST selectivity

ABSTRACT: The stability of microporous metal-organic frameworks (MOFs) in moist environments must be taken into consideration for their practical implementations, which is largely ignored thus far. Herein, we synthesized a new moisture stable Zn-MOF, **{[Zn_2(SDB)$_2$(L)$_2$].2DMA}$_n$**, **IITKGP-12**, by utilizing a bent organic linker 4,4′-sulfonyldibenzoic acid (H_2SDB) containing polar sulfone group (-SO_2) and a N, N-donor spacer (**L**) with a BET surface area of 216 m^2g^{-1}. This material displays greater CO_2 adsorption capacity over N_2 and CH_4 with high IAST selectivity which is also validated by breakthrough experiments with longer breakthrough times for CO_2. Most importantly, the separation performance is largely unaffected in presence of moisture of simulated flue gas stream. TPD analysis shows the ease of regeneration process and the performance was verified for multiple cycles. In order to understand the structure-function relationship at the atomistic level, GCMC calculation was performed indicating that the primary binding site for CO_2 is between the sulfone moieties in **IITKGP-12**. CO_2 is attracted to the bonded structure (V-shape) of the sulfone moieties in a perpendicular fashion where C_{CO2} is aligned with S and the CO_2 axis bisects the SO_2 axis. Thus, the strategic approach to immobilize the polar sulfone moiety with high number of inherent stronger M-N

coordination and the absence of coordination unsaturation made this MOF potential towards practical CO_2 separation applications.

INTRODUCTION

Metal-organic frameworks (MOFs)[1-4] are synthesized by reacting metal ions/clusters with organic ligands to form 2D and 3D structures possessing permanent porosity, extra-large surface areas, tunable pore size and pore chemistry. As a result of these properties, MOFs have shown significant potential for a myriad of applications involving gas storage,[5-10] gas separation,[11-14] catalysis[15-16] and proton conduction.[17-21] While several MOFs have shown potential for usage in gas separation and adsorbent based industrial purification systems, the stability of these materials in moist atmospheres plays a vital role and must be taken into consideration due to the presence of moisture in industrial emissions. In coal-fired power plants, moisture is considered as a main component of flue gas stream (8-10% H_2O) and thus should not be ignored when assessing candidate adsorbent materials for selective CO_2 sorption from flue gas. Similarly, moisture plays an important role in the purification of landfill gas. In order to deploy MOFs in CO_2 capture and separations, their stability under humid conditions will be essential as MOFs are prone to degrade in the presence of moisture.[22-25] Though a large number of applications of MOFs have been published and there have been extensive studies of their properties, there are very few reports where the moisture sensitivity and stability of these substances have been investigated. Apart from imidazolate based ZIFs, Zr(IV) based MOFs, MILs based on the trivalent metal ions and a few recently developed MOFs, most of the reported MOFs have been found to be unstable in presence of moisture.[22-25] Many MOFs with carboxylic acid based ligands which are coordinated to the metal centers, these MOFs are largely unstable in presence of moisture but it is observed that MOFs which are having nitrogen coordinated frameworks are more basic and have greater moisture stability.[26] The M-O bonds in a carboxylic acid containing MOFs are readily hydrolyzed in presence of moisture compared to a more stable M-N bonds. Also, the water molecules are having high affinity to the coordinatively unsaturated metal centers, which has detrimental effect to the stability of the MOFs but is favorable for high uptake capacity for preferred gases. Because of these limitations, great efforts need to be made towards development of moisture stable MOFs to compete with zeolites and activated carbons for such practical usages.

The adsorption of CO_2 to these substances is based upon two parameters: firstly, the adsorption energy and secondly, the polarity and geometry of the frameworks. The incorporation of polar groups within the framework has an advantageous effect on tailoring the framework structure and thus increasing the selectivity of adsorption.[27-28] Unsaturated metal sites can also greatly enhance the polarity of the frameworks and this has been proved to be a very efficient technique to increase the selective sorption of CO_2 with a large quadruple moment.[29-31] Shimizu and Chen *et al.* have demonstrated that there is a significant effect on selective CO_2 sorption when polar groups like $–NH_2$ and H_2O have been incorporated on the MOFs surface.[27,32] Although, a large number of other functionality such as –OH and $–SO_3H$ have been proven to be effective for CO_2 separation,[33-34] the effect of sulfone ($–SO_2$) immobilized onto the framework backbone for CO_2 separation is rarely explored[35-36] and remains elusive detailing the interaction of CO_2 gas molecules with sulfone moieties of frameworks at the molecular level. To the best of our knowledge, the $–SO_2$ functionalized ligand H_2SDB (4,4′-sulfonyldibenzoic acid) used in this study has never been strategically explored to construct MOFs showing its high CO_2 separation performance supported with direct interactions with the sulfone moiety at the atomistic level. Again, such a high separation performance should not compromise with the moisture stability of the constructed MOFs. The state-of-art material Mg-MOF-74 shows the benchmark CO_2 uptake capacity in dry condition but it is hydrolytically unstable which restricts its practical usage.[23]

Thus, a strategy to immobilize the polar sulfone moiety onto the pore surface with high number of inherent stronger M-N coordination in absence of coordination unsaturation might be helpful to overcome the above-mentioned difficulties. Herein, we designed and synthesized a new moisture stable microporous Zn-MOF, **{[Zn_2(SDB)$_2$(L)$_2$].2DMA}$_n$**, **IITKGP-12**, by utilizing a bent organic linker H_2SDB containing polar -SO_2 group and a linear N, N-donor spacer **L** (1, 4-bis(3-pyridyl)-2,3-diaza-1,3-butadiene) under room temperature reaction. The stronger M-N ligation without coordination unsaturation and presence of sulfone moieties served the aforementioned two purposes i.e. imparting moisture stability and enhancing CO_2 capture-separation ability of **IITKGP-12**. The gas sorption study on activated sample exhibits greater CO_2 uptake with the high IAST selectivity for flue gas (0.15 bar CO_2/0.85 bar N_2) and landfill gas mixtures (0.5 bar CO_2/0.5 bar CH_4) at ambient conditions. Besides, the dynamic breakthrough studies validate the separation performance under practical separation environment. Amounts of CO_2 adsorbed for binary gas mixtures are relatively high as projected

via IAST method and experimentally determined from breakthrough experiments. GCMC calculations clearly reveal that the primary binding site for CO_2 is between the sulfone moieties in **IITKGP-12**.

EXPERIMENTAL SECTION

Materials. The spacer **L** was prepared following our previous report.[37]

Preparation of {[$Zn_2(SDB)_2(L)_2$].2DMA}$_n$, IITKGP-12. $Zn(NO_3)_2.6H_2O$ (0.030 g, 0.1 mmol), H_2SDB (0.031 g, 0.1 mmol) and **L** (0.021 g, 0.1 mmol) were placed in a glass vial, dissolved with 4 mL DMA and stirred around 1 h. Then the solution was kept at room temperature for crystallization. Yellow thin crystals were obtained within 15 days. Elemental analysis, Calcd: C, 53.97%; H, 4.05%; N, 10.49%; S, 4.80%. Found: C, 53.89%; H, 4.11%; N, 10.19%; S, 4.67%. FTIR (cm^{-1}): 3436(b), 2930.2(w), 1653.5(s), 1625.6(s), 1566.3(s), 1486(s), 1426.7(s), 1395.3(m), 1364(s), 1301.2(s), 1193(s), 1158.1(s), 1123.3(m), 1098.8(s), 1060.5(s), 1015.1(s), 969.8(m), 872.1(m), 851.2(m), 809.3(m), 779.9(s), 743(s), 695.2(s), 655.8(m), 627.9(s), 586.1(w).

RESULTS AND DISCUSSION

X-ray diffraction study shows that **IITKGP-12** grows in the monoclinic system with $P2_1/n$ space group. The formula of this MOF is established as **{[$Zn_2(SDB)_2(L)_2$].2DMA}$_n$** based on TGA, elemental analysis and single crystal X-ray study. The asymmetric unit of **IITKGP-12** contains two Zn(II) ions, two SDB^{2-} ligands and two spacer **L**. Figure 1a depicts the core view circling Zn(II) centers with a distorted tetrahedral configuration via coordinating with two O-atoms (O1, O5) from two SDB^{2-} linkers, two N-atoms (N1, N5) from two **L** spacer. Both the carboxylate groups of SDB^{2-} ligand adopt same coordination mode (monodentate) (Figure 1a). Structural interpretation divulges a 2D network with stair like layers. The topological analysis for **IITKGP-12** reveals a ***sql*** topology (Figure 1b).[38] Figure 1c represents different 2D layers in AA stacking sequence. Figure 1d represents overall 2D structure, showing the channels of ~4.2 Å x 6.2 Å (taking into account van der Waals radii) decorated with polar $–SO_2$ functionality along crystallographic *'a'* axis. The framework gets stabilized through several intermolecular non-

bonding contacts among the integral units (Table S3, SI). Total void volume amounts to 1269 $Å^3$ per unit cell volume of 5754.5 $Å^3$ (22.1%) as calculated by PLATON program.[39]

PXRD pattern of fresh crystal is well matched with simulated pattern (Figure S1, SI), confirming bulk phase purity of this material. TGA performed under N_2 atmosphere showing a weight loss of 13.11% until 275 ^oC (Figure S3, SI), which agrees to the departure of two lattice DMA molecules (calcd 13.06 %), after that framework started to degrade upon further heating.

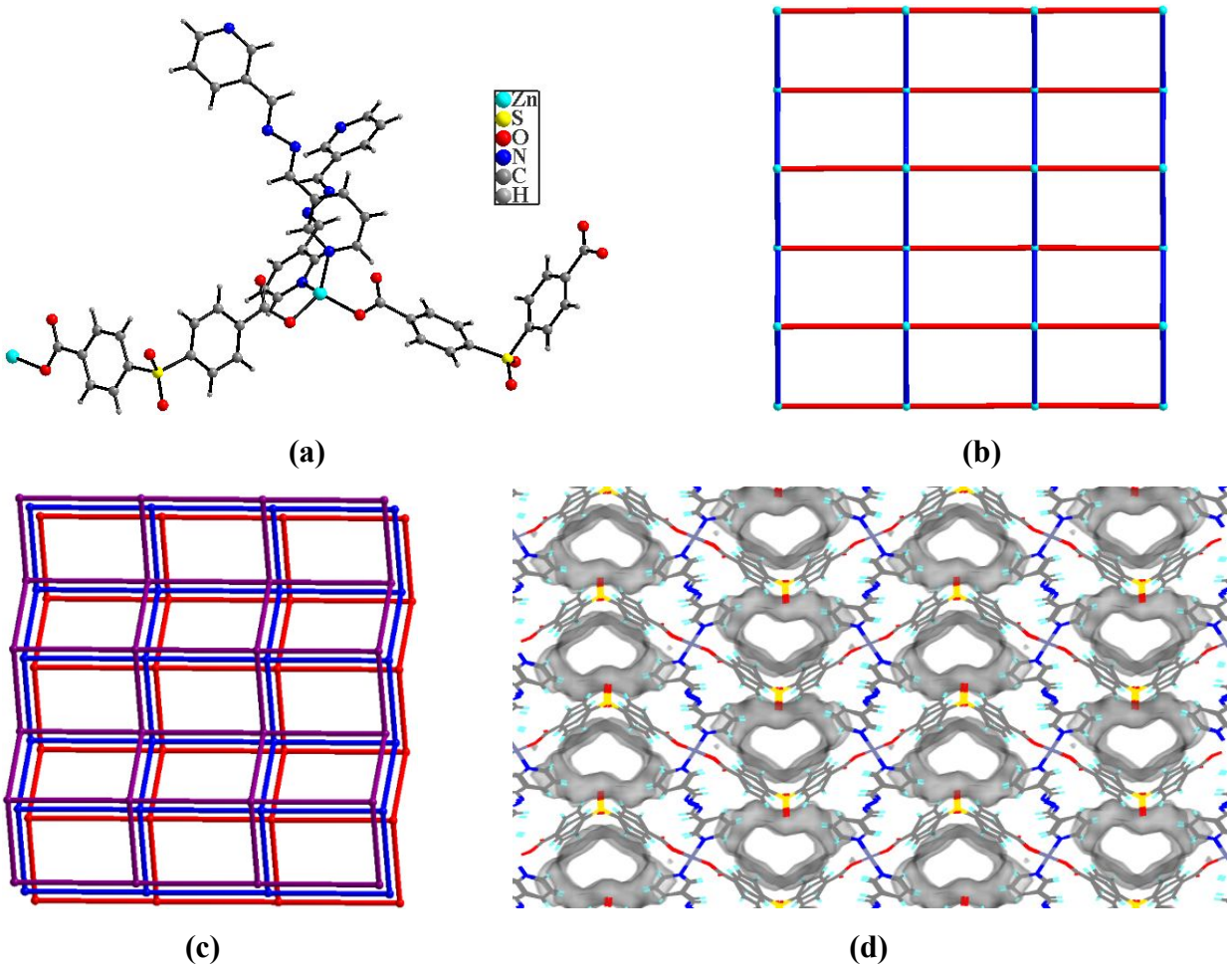

Figure 1. (a) View surrounding the Zn(II) cation in **IITKGP-12**. (b) A drawing of a 2D layer of ***sql*** topology. (c) Representation showing different 2D layers in AA stacking sequence. (d) A representation showing the micropores decorated with $–SO_2$ groups along crystallographic *'a'* axis in **IITKGP-12**.

Before evaluating **IITKGP-12** as a potential CO_2 capture adsorbent, first we explored its stability by taking PXRD data after exposure to 97% RH for 3-8 days (Figure 2), it could still maintain its structural integrity which indicates its excellent moisture stability. Moreover, we checked the PXRD pattern upon sample exposure to air for 40 days, which also shows the

preservation of the framework (Figure 2). Generally, it is known that only Zn-O coordinated MOFs are unstable in presence of moisture such as MOF-2 with ***sql*** topology.[40] Presence of two stronger M-N coordination bonds per metal center out of total four coordination sites and absence of removable coordinating solvent(s) in order to generate coordinatively unsaturated metal centers possibly makes **IITKGP-12** moisture stable.[23]

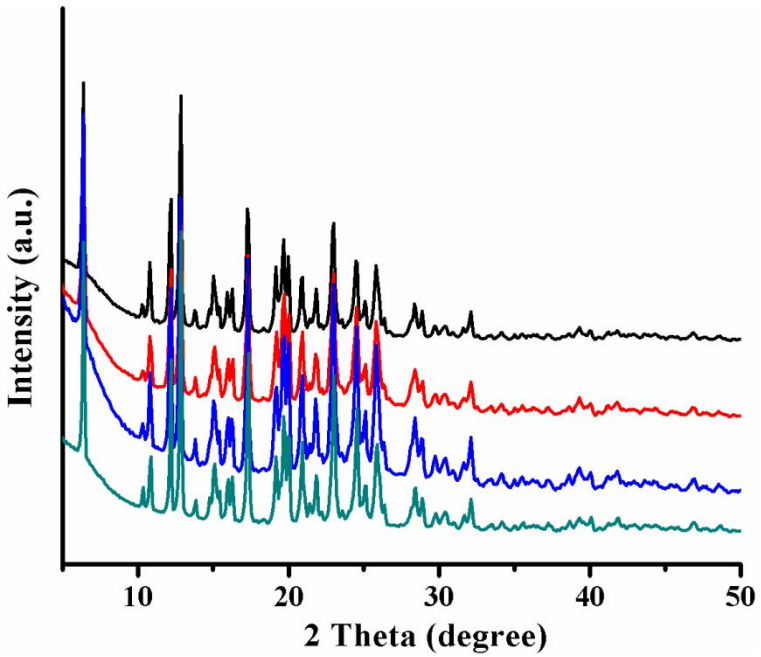

Figure 2. PXRD pattern of as-synthesized sample (dark cyan), after expose in 97% RH for 3 days (blue), after expose in 97% RH for 8 days (red) and after air exposure for 40 days (black).

Gas sorption studies are performed with the desolvated sample (**IITKGP-12a**) to check the permanent micro-porosity. The fresh crystals of MOF were dipped in dry $CHCl_3$ to eradicate lattice DMA solvents. The solvent exchanged crystals showed similar crystallinity as confirmed by recording the PXRD (Figure S2, SI). The exchanged material was degassed at 353 K for 10 h to obtain activated sample. **IITKGP-12a** maintains its structural integrity as confirmed from PXRD measurement (Figure S2, SI). This material does not uptake N_2 gas at 77 K which is also observed for many other micro-porous MOFs, indicating that the thermal energy of MOF and energy of adsorbate are insufficient to allow the diffusion of adsorbates through the micro pores.[41-42] CO_2 adsorption isotherm at 195 K shows the BET surface area of 216 m^2g^{-1} (Figure S4, SI). Gas adsorption isotherms for CO_2, CH_4 and N_2, executed on **IITKGP-12a** at 273 and 295K are depicted in Figure 3a and 3b, respectively. It exhibits higher CO_2 uptake over CH_4 and

N_2. The uptake capacity of CO_2 amounts to 2.26 mmolg^{-1} (9.96 wt%) and 2.004 mmolg^{-1} (8.82 wt%) at 273 and 295 K respectively, under 1 bar. In contrast, at 1 bar, it adsorb much lower quantity of CH_4: 1.2 mmolg^{-1} (1.92 wt%) at 273 K, 0.93 mmolg^{-1} (1.48 wt%) at 295 K and N_2: 0.44 mmolg^{-1} (1.23 wt%) at 273 K; 0.34 mmolg^{-1} (0.94 wt%) at 295 K. Such highly selective CO_2 uptake might be due to existence of polar sulfone group on the backbone of **IITKGP-12**, which interacts more strongly with CO_2 having a large quadruple moment.

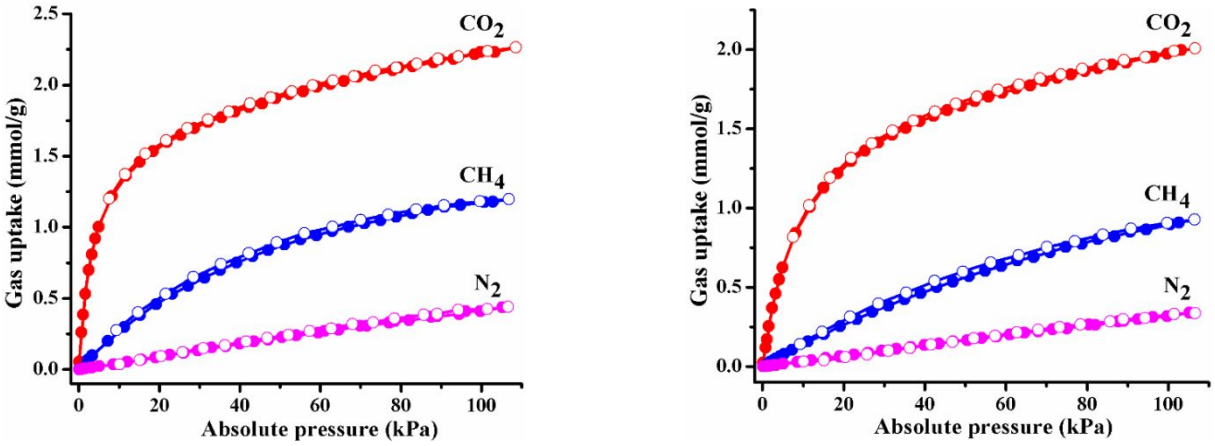

Figure 3. Gas adsorption isotherms (a) at 273 K and (b) at 295 K by **IITKGP-12a** (filled/empty symbols: adsorption/desorption).

To examine the affinity of **IITKGP-12a** towards the gases, isosteric adsorption enthalpies (Q_{st}) were assessed from single-component isotherms by using Clausius–Clapeyron equation. At near zero coverage the Q_{st} values are 35.2, 22.6 and 11.2 kJmol^{-1} for CO_2, CH_4 and N_2, respectively, (Figure S5, SI) demonstrating the attraction of gases towards the framework in the descending order of CO_2>CH_4>N_2. We also calculated the Q_{st} for CO_2, CH_4 and N_2 adsorption via virial method and the results from virial method are correlating well with the Clausius-Clapeyron method (Figure S7, SI). Q_{st} of CO_2 is similar/higher to the values for HKUST (35 kJmol^{-1}),[43] IITKGP-8 (35 kJmol^{-1}),[44] ZIF-78 (29 kJmol^{-1}),[45] SIFSIX-2-Cu (22 kJmol^{-1}),[46] SIFSIX-2-Cu-i (31.9 kJmol^{-1}),[46] UTSA-16 (34.6 kJmol^{-1}),[32] UTSA-15a (28.6 kJmol^{-1}),[32] UTSA-20a (32.4 kJmol^{-1}),[32] UTSA-33a (30 kJmol^{-1}),[32] UTSA-49 (27 kJmol^{-1}),[47] [Cu(bcppm)H_2O] (29 kJmol^{-1}),[48] ZTF-1 (25.4 kJ/mol),[49] IITKGP-6 (23 kJmol^{-1}).[35] This notably moderate Q_{st} value for CO_2 compared to the liquid amines for CO_2 chemisorption (105 kJmol^{-1})

and MOFs with Q_{st} higher than 45 kJmol^{-1} ensures the facile regeneration process of the material potential for practical separation of CO_2 from its gas mixtures.

Because of the discrimination in its uptake capacities, we assessed the gas separation selectivity of binary gas mixtures at different temperatures. Ideal adsorbed solution theory (IAST)[50] was applied to determine the sorption selectivity of **IITKGP-12a** for 15:85 (v/v) CO_2/N_2 (flue gas) and 50:50 (v/v) CO_2/CH_4 (biogas) gas mixtures at 273 and 295K. The dual-site Langmuir-Freundlich (DSLF) equation was employed for fitting the isotherms data (Figures S8-S9, SI). The fitting parameters were used to acquire the multi-component sorption isotherms via IAST method (Table S4, SI). The IAST selectivity results under 1 bar are shown in Figure 4 ((CO_2/N_2: 75 (273 K) and 40 (295 K); CO_2/CH_4: 15 (273 K) and 12 (295 K)). We also calculated the IAST selectivity using the dual-site Langmuir (DSL) fittings, showing similar results with DSLF fittings (Figure S12, SI). These values are upper side or comparable to those of many well-known MOFs: TIFSIX-1-Cu, SIFSIX-1-Cu, SIFSIX-2-Cu, PCN-61, PCN-88, $Cu_{24}(TPBTM)_8$, MOF-177, HKUST-1, Cu-BTTri, en-Cu-BTTri, UTSA-72a, Zn-MOF-74 and zeolites (MFI, 13X) (Table S5, SI),[32,46-47,51-56] and thus demonstrating the prospective of **IITKGP-12** towards such important gas separations.

It is important to consider the uptake amounts of the desired gas from binary gas mixtures while a specific material is projected for its practical usage. Thus, simultaneously high selectivity and high uptake capacity are desirable for such practical purposes. Therefore, we calculated the loading amounts of CO_2 through IAST method under 100 kPa pressure for CO_2/N_2 and CO_2/CH_4 gas mixtures at 273 and 295 K (Figure 4). CO_2 loadings from CO_2/N_2 (15:85) mixture amount to 1.38 mmolg^{-1} (273 K) and 1.06 mmolg^{-1} (295 K). The value 1.06 mmolg^{-1} is considerably larger than zeolite MFI (0.26 mmolg^{-1}), ZIF-78 (0.76 mmolg^{-1}) and MOF-177 (0.16 mmolg^{-1}) under similar condition.[32] The mixed gas uptake amounts are calculated to be 1.82 mmolg^{-1} (273 K) and 1.55 mmolg^{-1} (295 K) for CO_2/CH_4 (50:50) mixture, which are found to be greater than IITKGP-8 (0.55 mmolg^{-1} at 295 K)[44] and IITKGP-6 (1.54 and 0.77 mmolg^{-1} at 273 and 295 K).[35]

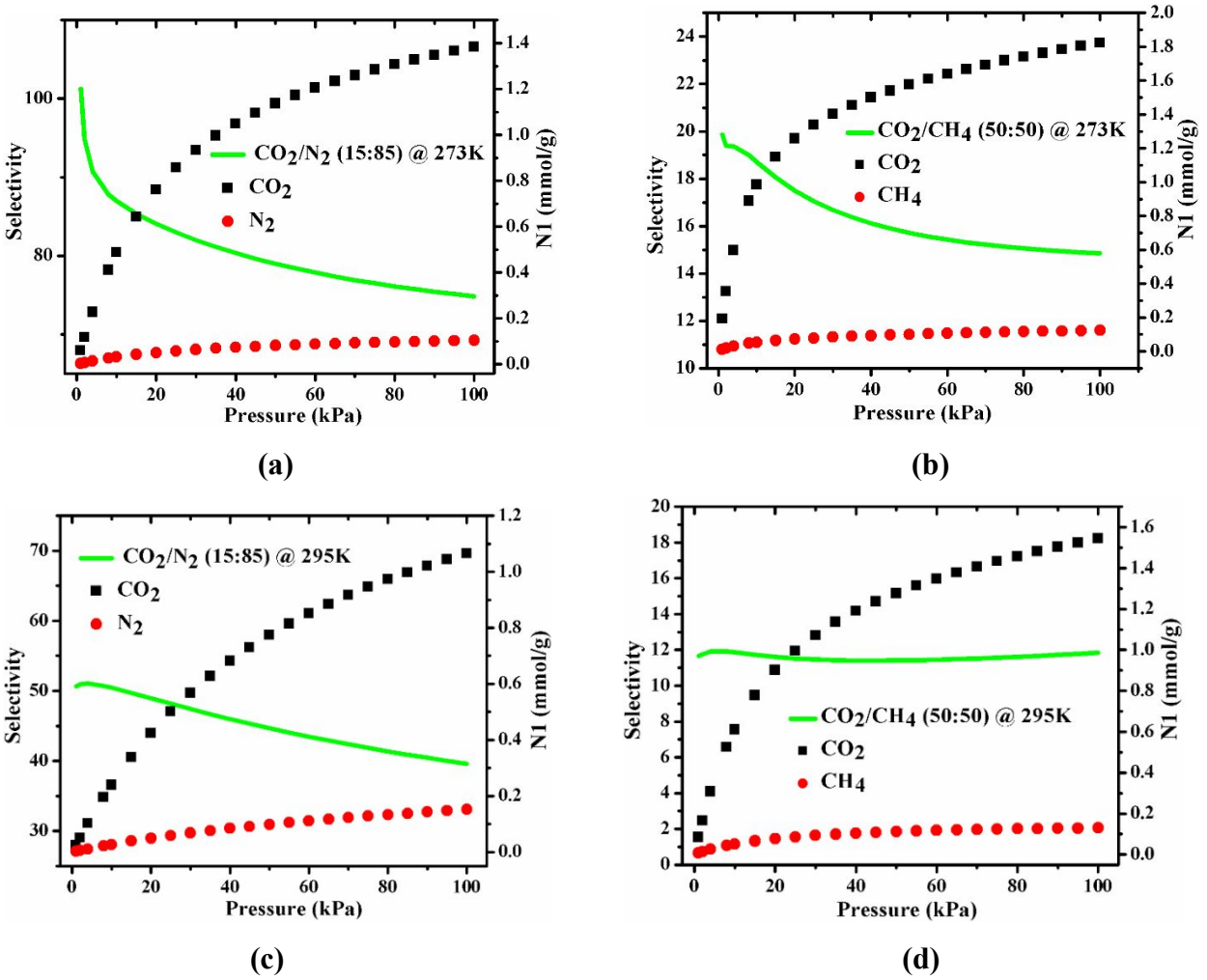

Figure 4. Binary mixture gas sorption isotherms and gas separation selectivities at 273 K (a, b); at 295 K (c, d); calculated by IAST method for CO_2/N_2 (15:85) and CO_2/CH_4 (50:50) gas mixtures.

Dynamic breakthrough study:

To further examine the practical CO_2 separation performance of **IITKGP-12a**, dynamic breakthrough experiments were conducted using CO_2/N_2 (dry and wet) and CO_2/CH_4 gas mixtures at 295 K/1 bar. Gas mixtures that simulated flue gas (CO_2/N_2, 15:85, dry and wet) and landfill gas (CO_2/CH_4, 50:50) were passed through a fixed bed reactor (6 mm Ø, total flow: 2 cm^3/min) filled with activated sample (Figure S13, SI). Before breakthrough experiments, the sample were heated at 333 K for 3 h under He gas flow to eliminate atmospheric impurities before being cooled down to room temperature. The outlet gas composition was constantly examined by a mass spectrometer (see SI). N_2 and CH_4 gas were found to be quickly eluted through the sample bed which suggests that the co-adsorption of these gases was negligible

(Figure 5). CO_2 breakthrough occurred approximately at 98, 78 and 36 min after exposure to gas mixtures of dry and wet CO_2/N_2 and dry CO_2/CH_4, respectively. CO_2 breakthrough times for these gas mixtures were found to be parallel to some famous MOFs as listed in Table S6, SI.[46,57-65] Upon achieving equilibrium, regeneration experiments were performed upon **IITKGP-12a**. It should be noted that it could be easily regenerated by degassing under a He flow at 295 K for 15 min for dry gas mixtures. When **IITKGP-12a** was exposed to moist gas mixtures, complete regeneration was found to be possible by heating to moderate temperatures (333 K, 30 min) during temperature programmed desorption (TPD) experiments (Figure S14). Cycling experiments found that **IITKGP-12a** maintained this sorption performance over four successive adsorption/desorption cycles (Figure S15).

CO_2 adsorption capacity of **IITKGP-12a** was calculated to be 1.29, 0.94 and 1.65 $mmolg^{-1}$ for the three gas mixtures respectively, under these dynamic conditions (Table 1). It is worthy to mention that these loading amounts in the mixed gas phases for dry gas mixtures are equivalent to the values found from IAST method (1.06 and 1.55 $mmolg^{-1}$ for CO_2/N_2 and CO_2/CH_4, respectively at 295K, Table 1). The separation selectivity of the gas mixtures are 163, 119 and 37 for dry CO_2/N_2, wet CO_2/N_2 and CO_2/CH_4 respectively. The breakthrough performance of this material illustrates the limitations of IAST calculations as this method estimates selectivity from single component adsorption isotherms at equilibrium, something which has been observed in a number of previous reports.[66-67] Breakthrough experiments enable the study of gas separation performance under dynamic conditions which illustrate the effects of uptake kinetics, inter-particle diffusivity and mass transfer through packed beds all of which can account for the difference between IAST predicted uptake and experimental breakthrough study results.

It may be noted that a slightly reduced separation selectivity and CO_2 loading amounts in the mixed phase could be observed while humidity is considered and thus making this material as a potential candidate for such type of practical gas separation application. Despite the absence of open metal sites (OMS) in **IITKGP-12a**, the materials still exhibits a slight reduction in performance in presence of moisture as seen in the wet CO_2/N_2 breakthrough experiment (Figure 5). This can be attributed to the highly polar nature on H_2O molecules which may form hydrogen bonds with exposed H and O atoms of the framework, which in turn gives way to competitive adsorption and slightly reduced CO_2 uptake under moist conditions. Several studies have

confirmed that the existence of moisture in the mixed gas system has a negative influence on M/MOF-74 materials for CO_2 adsorption potential,[68] particularly introduction to 70% RH in CO_2/N_2 gas stream showed marked decrease in breakthrough separation performance for all the variations.[69] On the other hand, the well-known SIFSIX-3-Zn and SIFSIX-2-Cu-i MOFs displayed a slight reduction in breakthrough separation performance in the existence of 74% RH for CO_2/N_2 binary mixtures.[46]

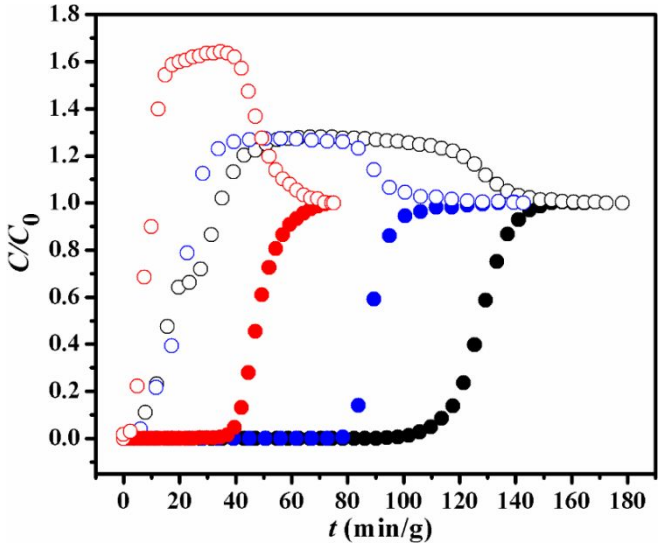

Figure 5. Breakthrough curves for **IITKGP-12a** in a fixed-bed under flow (2 cm^3/min) of CO_2/CH_4 (50/50, red) and CO_2/N_2 (15/85) gas mixtures under dry (black) and wet (blue) (74% humidity) environments. Filled circles = CO_2, empty circles = CH_4 or N_2.

Table 1: Amount of CO_2 and N_2 adsorbed in binary gas phase and selectivity data from both Breakthrough experiments and IAST method at 295 K/1 bar.

Binary gas mixtures at 295 K	Breakthrough experiments selectivity	IAST selectivity	Amount of CO_2 adsorbed from Breakthrough experiments ($mmolg^{-1}$)	Amount of CO_2 adsorbed from IAST method ($mmolg^{-1}$)	Amount of N_2 adsorbed from Breakthrough experiments ($mmolg^{-1}$)	Amount of N_2 adsorbed from IAST method ($mmolg^{-1}$)
Dry CO_2/N_2 (15/85)	163	40	1.29	1.06	0.045	0.152
Wet CO_2/N_2 (15/85)	119	-	0.94	-	0.046	-
Dry CO_2/CH_4 (50/50)	37	12	1.65	1.55		

Molecular simulation:

To understand the sorption behavior in **IITKGP-12**, Grand Canonical Monte Carlo (GCMC) molecular calculations of CO_2 sorption were performed (see SI). Histogram of CO_2 loading from GCMC simulation at 0.05 atm and 295 K shows that there are 32 optimal occupation sites per unit cell (Figure S18, SI). The population of CO_2 is high between neighboring sulfone moieties. There is a cooperative effect from adjacent sulfone groups to make highly favorable periodic pockets for CO_2 sorption. Radial distribution comparison at 0.05 atm and 1.0 atm at 295 K (Figure S19, SI) also shows that with increasing pressure, the CO_2 molecules move closer to sulfone groups in **IITKGP-12**. The initial peak for the strongest interaction is 4.24 Å for 0.05 atm and 3.92 Å at 1.0 atm. The primary binding site for CO_2 is between the sulfone moieties in **IITKGP-12**. CO_2 is attracted to the bonded structure (V-shape) of the sulfone moieties in a perpendicular fashion; C_{CO2} is aligned with S, the CO_2 axis bisects the SO_2 axis. The interaction distances between C_{CO2} and O(MOF) from sulfone groups are 2.94 and 4.20 Å as shown in Figure 6. Van der Waals and electrostatic attraction of the sulfone O atoms to the electropositive C_{CO2} is the primary cause of physisorption. Percent contributions of the potential energy for this binding site are: 64.9% repulsion-dispersion, 30.1% electrostatics, and 5.0% polarization. The binding energy was calculated to be 35.07 $kJmol^{-1}$ (Figure S17, SI), correlating well with the experimental Q_{st} (35.2 $kJmol^{-1}$) obtained from Clausius–Clapeyron equation. However, the Q_{st} slope is approximately zero, suggesting uniform binding sites throughout the crystal and minimal or no cooperative loading of CO_2 molecules. GCMC simulated CO_2 adsorption isotherms under 1 bar (Figure S16, SI) show the uptake amounts at 273 and 295 K are 2.36 and 2.02 $mmolg^{-1}$, respectively, which are in well agreement with the experimental isotherms (2.26 and 2.004 $mmolg^{-1}$, respectively).

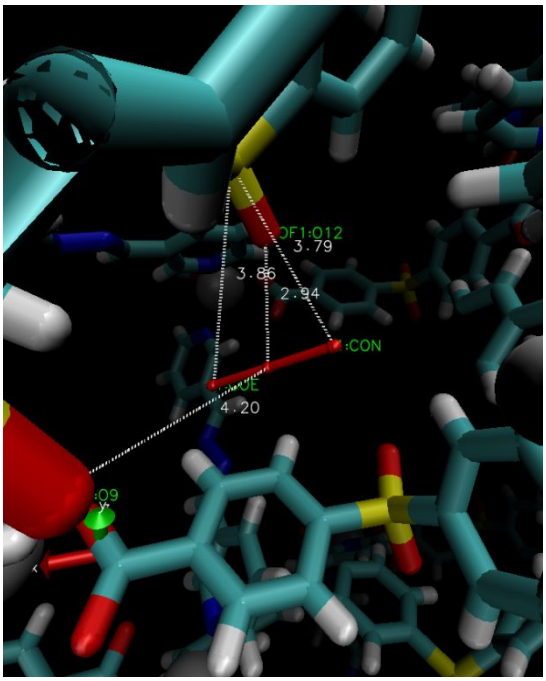

Figure 6. Binding interaction distances for adsorbed CO_2 and the sulfone moieties in **IITKGP-12**. Left O-S interaction: 3.86 Å, middle-bottom C-O interaction: 4.20 Å, middle-top C-O interaction: 2.94 Å, right O-S interaction: 3.79 Å. Average interaction distance: 3.70 Å.

CONCLUSION:

In summary, we have taken up a strategic approach to induce moisture stability and high CO_2 binding affinity and hence separation selectivity exhibited by a 2D microporous Zn-MOF based on bent organic linker and a N, N-donor spacer **L** consisting a channel of ~4.2 Å x 6.2 Å decorated with polar -SO_2 functionality along crystallographic *'a'* axis. Gas sorption experiments displayed selective CO_2 capture over N_2 and CH_4. GCMC calculations on CO_2 adsorption showed that CO_2 molecules are attracted to the bonded structure (V-shape) of the sulfone moieties in a perpendicular fashion. At ambient conditions, high CO_2/N_2 and CO_2/CH_4 selectivities were accomplished both from IAST method and real time breakthrough studies with considerably greater CO_2 uptakes in binary gas mixtures. Most importantly, the separation performance is largely unaffected in presence of moisture of simulated flue gas stream. TPD analysis and recycling experiments have shown the ease of its regeneration and the usage over multiple cycles for such separations. Besides, moisture stability of this microporous MOF is an attractive feature that makes it a promising candidate for such important gas separations. Our study may find useful for developing the design principles for future synthetic efforts of humid stable MOFs for various adsorption-based applications.

ASSOCIATED CONTENT

Supporting Information (SI)

Instrument details, X-ray crystallographic parameters, calculation of the cost of the MOF, PXRD plots, TGA plot, Q_{st} calculation, IAST calculations, fitting plots, table of fitting parameters and IAST selectivity, breakthrough experiments details, TPD experiment details, GCMC simulation details. CCDC 1956987.

Corresponding Author

*E-mail: mcdas@chem.iitkgp.ac.in

ORCID[iD]

Madhab C. Das: 0000-0002-6571-8705
David G. Madden: 0000-0003-3875-9146
Arun Pal: 0000-0002-0665-3446

Acknowledgments

A.P. acknowledges UGC for the research fellowship. M.C.D. acknowledges the SERB, New Delhi as Core Research Grant (CRG/2019/001034) and the DST, New Delhi (DST/TM/EWO/MI/CCUS/21) for financial support. B. S. acknowledges the National Science Foundation (Award No. DMR-1607989), including support from the Major Research Instrumentation Program (Award No. CHE-1531590). Computational resources were made available by an XSEDE Grant (No. TG-DMR090028) and Research Computing at the University of South Florida.

References

1. Li, H.; Eddaoudi, M.; O'Keeffe, M.; Yaghi, O. M. Design and Synthesis of an Exceptionally Stable and Highly Porous Metal-organic Framework. *Nature* **1999**, *402*, 276-279.
2. Eddaoudi, M.; Kim, J.; Rosi, N.; Vodak, D.; Wachter, J.; O'Keeffe, M.; Yaghi, O. M. Systematic Design of Pore Size and Functionality in Isoreticular MOFs and Their Application in Methane Storage. *Science* **2002**, *295*, 469-472.
3. Yaghi, O. M.; O'Keeffe, M.; Ockwig, N. W.; Chae, H. K.; Eddaoudi, M.; Kim, J. Reticular Synthesis and the Design of New Materials. *Nature* **2003**, *423*, 705-714.
4. Special Issue on MOF: Zhou, H. -C.; Long, J. R.; Yaghi, O. M. Introduction to Metal−Organic Frameworks. *Chem. Rev*. **2012**, *112*, 673-674.
5. Themed collection on MOF: Li, J.-R.; Kuppler, R. J.; Zhou, H. -C. Selective Gas Adsorption and Separation in Metal–organic Frameworks. *Chem. Soc. Rev*. **2009**, *38*, 1477-1504.
6. Deria, P.; Mondloch, J. E.; Karagiaridi, O.; Bury, W.; Hupp, J. T.; Farha, O. K. Beyond Post-synthesis Modification: Evolution of Metal–organic Frameworks via Building Block Replacement. *Chem. Soc. Rev*. **2014**, *43*, 5896-5912.
7. Nandi, S.; Collins, S.; Chakraborty, D.; Banerjee, D.; Thallapally, P. K.; Woo, T. K.; Vaidhyanathan, R. Ultralow Parasitic Energy for Postcombustion CO_2 Capture Realized

in a Nickel Isonicotinate Metal−Organic Framework with Excellent Moisture Stability. *J. Am. Chem. Soc.* **2017**, *139*, 1734-1737.

8. Chen, Z.; Li, P.; Anderson, R.; Wang, X.; Zhang, X.; Robison, L.; Redfern, L. R.; Moribe, S.; Islamoglu, T.; Gómez-Gualdrón, D. A.; Yildirim, T.; Stoddart, J. F.; Farha, O.K. Balancing Volumetric and Gravimetric Uptake in Highly Porous Materials for Clean Energy. *Science* **2020**, *368,* 297-303.
9. Murray, L. J.; Dincă, M.; Long, J. R. Hydrogen Storage in Metal−organic Frameworks. *Chem. Soc. Rev*. **2009**, *38*, 1294−1314.
10. Xue, D. –X.; Cairns, A. J.; Belmabkhout, Y.; Wojtas, L.; Liu, Y.; Alkordi, M. H.; Eddaoudi, M. Tunable Rare-Earth fcu-MOFs: A Platform for Systematic Enhancement of CO_2 Adsorption Energetics and Uptake. *J. Am. Chem. Soc.* **2013**, *135*, 7660−7667.
11. Lin, R. -B.; Xiang, S.; Xing, H.; Zhou, W.; Chen, B. Exploration of Porous Metal–organic Frameworks for Gas Separation and Purification. *Coord. Chem. Rev*. **2019**, *378*, 87–103.
12. He, Y.; Zhou, W.; Qian, G.; Chen, B. Methane Storage in Metal−organic Frameworks. *Chem. Soc. Rev*. **2014**, *43*, 5657-5678.
13. Bhatt, P. M.; Belmabkhout, Y.; Cadiau, A.; Adil, K.; Shekhah, O.; Shkurenko, A.; Barbour, L. J.; Eddaoudi, M. A Fine-Tuned Fluorinated MOF Addresses the Needs for Trace CO_2 Removal and Air Capture Using Physisorption. *J. Am. Chem. Soc.* **2016**, *138*, 9301−9307.
14. Goswami, R.; Seal, N.; Dash, S. R.; Tyagi, A.; Neogi, S. Devising Chemically Robust and Cationic Ni(II)-MOF with Nitrogen-Rich Micropores for Moisture-Tolerant CO_2 Capture: Highly Regenerative and Ultrafast Colorometric Sensor for TNP and Multiple Oxo-Anions in Water with Theoretical Revelation. *ACS Appl. Mater. Interfaces* **2019**, *11*, 40134-40150.
15. Yoon, M.; Srirambalaji, R.; Kim, K. Homochiral Metal−Organic Frameworks for Asymmetric Heterogeneous Catalysis. *Chem. Rev*. **2012**, *112*, 1196−1231.
16. Lee, J.; Farha, O. K.; Roberts, J.; Scheidt, K. A.; Nguyen, S. T.; Hupp, J. T. Metal−Organic Framework Materials as Catalysts. *Chem. Soc. Rev*. **2009**, *38*, 1450−1459.
17. Chand, S.; Elahi, S. M.; Pal, A.; Das, M. C. Metal Organic Frameworks and Other Crystalline Materials for Ultrahigh Superprotonic Conductivities of 10^{-2} S cm^{-1} or Higher. *Chem. Eur. J*. **2019**, *25*, 6259-6269.
18. Lim, D.-W.; Sadakiyo, M.; Kitagawa, H. Proton Transfer in Hydrogen-bonded Degenerate Systems of Water and Ammonia in Metal–organic Frameworks. *Chem. Sci.* **2019**, *10*, 16–33.
19. Elahi, S. M.; Chand, S.; Deng, W. -H.; Pal, A.; Das, M. C. Polycarboxylates Templated Coordination Polymers: Role of Templates for Superprotonic Conductivities up to 10^{-1} S cm^{-1}. *Angew. Chem. Int. Ed.* **2018**, *57*, 6662-6666.
20. Pal, S. C.; Chand, S.; Kumar, A. G.; Mileo, P. G. M.; Silverwood, I.; Maurin, G.; Banerjee, S.; Elahi, S. M.; Das, M. C. A Co(II)-Coordination Polymer for Ultrahigh Superprotonic Conduction: An atomistic Insight through Molecular Simulations and QENS Experiments. *J. Mater. Chem. A* **2020**, *8*, 7847–7853.
21. Pal, A.; Pal, S. C.; Otsubo, K.; Lim, D. -W.; Chand, S.; Kitagawa, H.; Das, M. C. A Phosphate-Based Silver-Bipyridine 1D Coordination Polymer with Crystallized Phosphoric acid as Superprotonic Conductor. *Chem. Eur. J*. **2020**, *26*, 4607-4612.

22. Wang, C.; Liu, X.; Demir, N. K.; Ceogihen, J. P.; Li, K. Applications of Water Stable Metal–Organic Frameworks. *Chem. Soc. Rev.* **2016**, *45*, 5107-5134.
23. Burtch, N. C.; Jasuja, H.; Walton, K. S. Water Stability and Adsorption in Metal−Organic Frameworks. *Chem. Rev*. **2014**, *114*, 10575−10612.
24. Canivet, J.; Fateeva, A.; Guo, Y.; Coasne, B.; Farrusseng, D. Water Adsorption in MOFs: Fundamentals and Applications. *Chem. Soc. Rev.* **2014**, *43*, 5594−5617.
25. Kumar, A.; Madden, D. G.; Lusi, M.; Chen, K. -J.; Daniels, E. A.; Curtin, T.; Perry IV, J. J.; Zaworotko, M. J. Direct Air Capture of CO_2 by Physisorbent Materials. *Angew. Chem. Int. Ed.* **2015**, *54*, 14372 –14377.
26. Jasuja, H.; Huang, Y.-G.; Walton, K. S. Adjusting the Stability of Metal−Organic Frameworks under Humid Conditions by Ligand Functionalization. *Langmuir* **2012**, *28*, 16874−16880.
27. Vaidhyanathan, R.; Iremonger, S. S.; Shimizu, G. K. H.; Boyd, P.G.; Alavi, S.; Woo, T. K. Direct Observation and Quantification of CO_2 Binding Within an Amine-Functionalized Nanoporous Solid. *Science* **2010**, *330*, 650-653.
28. Lu, W.; Verdegaal, W. M.; Yu, J.; Balbuena, P. B.; Jeong, H. -K.; Zhou, H. –C. Building Multiple Adsorption Sites in Porous Polymer Networks for Carbon Capture Applications. *Energy Environ. Sci*. **2013**, *6*, 3559-3564.
29. Dietzel, P. D. C.; Johnsen, R. E.; Fjellvåg, H.; Bordiga, S.; Groppo, E.; Chavan, S.; Blom, R. Adsorption Properties and Structure of CO_2 Adsorbed on Open Coordination Sites of Metal–organic Framework Ni_2(dhtp) from Gas Adsorption, IR Spectroscopy and X-ray Diffraction. *Chem. Commun*. **2008**, 5125–5127.
30. Yu, J.; Xie, L.-H.; Li, J.-R.; Ma, Y.; Seminario, J. M.; Balbuena, P. B. CO_2 Capture and Separations Using MOFs: Computational and Experimental Studies. *Chem. Rev.* **2017**, *117*, 9674−9754.
31. Queen, W. L.; Brown, C. M.; Britt, D. K.; Zajdel, P.; Hudson, M. R.; Yaghi, O. M. Site-Specific CO_2 Adsorption and Zero Thermal Expansion in an Anisotropic Pore Network. *J. Phys. Chem. C* **2011**, *115*, 24915–24919.
32. Xiang, S.; He, Y.; Zhang, Z.; Wu, H.; Zhou, W.; Krishna, R.; Chen, B. Microporous Metal-organic Framework with Potential for Carbon Dioxide Capture at Ambient Conditions. *Nat. Commun*. **2012**, *3*, 954-963.
33. Yang, S.; Sun, J.; Ramirez-Cuesta, A. J.; Callear, S. K.; David, W. I. F.; Anderson, D. P.; Newby, R.; Blake, A. J.; Parker, J. E.; Tang, C. C.; Schröder, M. Selectivity and Direct Visualization of Carbon Dioxide and Sulfur Dioxide in a Decorated Porous Host. *Nat. Chem.* **2012**, *4*, 887-894.
34. Yang, Q.; Wiersum, A. D.; Llewellyn, P. L.; Guillerm, V.; Serre, C.; Maurin, G. Functionalizing Porous Zirconium Terephthalate UiO-66(Zr) for Natural Gas Upgrading: a Computational Exploration. *Chem. Commun*. **2011**, *47*, 9603–9605.
35. Pal, A.; Chand, S.; Das, M. C. A Water-Stable Twofold Interpenetrating Microporous MOF for Selective CO_2 Adsorption and Separation. *Inorg. Chem.* **2017**, *56*, 13991-13997.
36. Wang, B.; Huang, H.; Lv, X. -L.; Xie, Y.; Li, M.; Li, J. -R. Tuning CO_2 Selective Adsorption over N_2 and CH_4 in UiO-67 Analogues through Ligand Functionalization. *Inorg. Chem.* **2014**, *53*, 9254−9259.
37. Pal, A.; Chand, S.; Senthilkumar, S.; Neogi, S.; Das, M. C. Structural Variation of Transition Metal Coordination Polymers based on Bent Carboxylate and Flexible Spacer

Ligand: Polymorphism, Gas Adsorption and SC-SC Transmetallation. *CrystEngComm* **2016**, *18*, 4323-4335.
38. Blatov, V. A. IUCr CompComm Newsletter, **2006**, vol. *7*, p. 4; http://www.topos.ssu.samara.ru.
39. Platon Program: Spek, A. L. *Acta Crystallogr. Sect. A* **1990**, *46*, 194-201.
40. Li, H.; Eddaoudi, M.; Groy, T. L.; Yaghi, O. M. Establishing Microporosity in Open Metal-Organic Frameworks: Gas Sorption Isotherms for Zn(BDC) (BDC = 1,4-Benzenedicarboxylate). *J. Am. Chem. Soc.* **1998**, *120,* 8571-8572.
41. Maji, T. K.; Matsuda, R.; Kitagawa, S. A Flexible Interpenetrating Coordination Framework with a Bimodal Porous Functionality. *Nat. Mater.* **2007**, *6*, 142-148.
42. Das, M. C.; Guo, Q.; He, Y.; Kim, J.; Zhao, C.-G.; Hong, K.; Xiang, S.; Zhang, Z.; Thomas, K. M.; Krishna, R.; Chen, B. Interplay of Metalloligand and Organic Ligand to Tune Micropores within Isostructural Mixed-Metal Organic Frameworks (M′MOFs) for Their Highly Selective Separation of Chiral and Achiral Small Molecules. *J. Am. Chem. Soc.* **2012**, *134*, 8703–8710.
43. Liang, Z.; Marshall, M.; Chaffee, A. L. CO_2 Adsorption-Based Separation by Metal Organic Framework (Cu-BTC) versus Zeolite (13X). *Energy Fuels* **2009**, *23*, 2785–2789.
44. Chand, S.; Pal, A.; Das, M. C. A Moisture-Stable 3D Microporous Co^{II}-Metal–Organic Framework with Potential for Highly Selective CO_2 Separation under Ambient Conditions. *Chem. Eur. J.* **2018**, *24*, 5982-5986.
45. Phan, A.; Doonan, C. J.; Uribe-Romo, F. J.; Knobler, C. B.; O'Keeffe, M.; Yaghi, O. M. Synthesis, Structure, and Carbon Dioxide Capture Properties of Zeolitic Imidazolate Frameworks. *Acc. Chem. Res*. **2010**, *43*, 58-67.
46. Nugent, P.; Belmabkhout, Y.; Burd, S. D.; Cairns, A. J.; Luebke, R.; Forrest, K.; Pham, T.; Ma, S.; Space, B.; Wojtas, L.; Eddaoudi, M.; Zaworotko, M. J. Porous Materials with Optimal Adsorption Thermodynamics and Kinetics for CO_2 Separation. *Nature* **2013**, *495*, 80-84.
47. Xiong, S.; Gong, Y.; Wang, H.; Wang, H.; Liu, Q.; Gu, M.; Wang, X.; Chen, B.; Wang, Z. A New Tetrazolate Zeolite-like Framework for Highly Selective CO_2/CH_4 and CO_2/N_2 Separation. *Chem. Commun*. **2014**, *50*, 12101-12104.
48. Bloch, W. M.; Babarao, R.; Hill, M. R.; Doonan, C. J.; Sumby, C. J. Post-synthetic Structural Processing in a Metal–Organic Framework Material as a Mechanism for Exceptional CO_2/N_2 Selectivity. *J. Am. Chem. Soc.* **2013**, *135*, 10441–10448.
49. Panda, T.; Pachfule, P.; Chen, Y.; Jiang, J.; Banerjee, R. Amino Functionalized Zeolitic Tetrazolate Framework (ZTF) with High Capacity for Storage of Carbon Dioxide. *Chem. Commun*. **2011**, *47*, 2011-2013.
50. Myers, A. L.; Prausnitz, J. M. Thermodynamics of Mixed-gas Adsorption. *AIChE J.* **1965**, *11*, 121-127.
51. Nugent, P.; Rhodus, V.; Pham, T.; Tudor, B.; Forrest, K.; Wojtas, L.; Space, B.; Zaworotko, M. Enhancement of CO_2 Selectivity in a Pillared *pcu* MOM Platform through Pillar Substitution. *Chem. Commun*. **2013**, *49*, 1606-1608.
52. Zheng, B.; Bai, J.; Duan, J.; Wojtas, L.; Zaworotko, M. J. Enhanced CO_2 Binding Affinity of a High-Uptake *rht*-Type Metal−Organic Framework Decorated with Acylamide Groups. *J. Am. Chem. Soc*. **2011**, *133*, 748-751.

53. Li, J. -R.; Yu, J.; Lu, W.; Sun, L.-B.; Sculley, J.; Balbuena, P. B.; Zhou, H.-C. Porous Materials with Pre-designed Single-molecule Traps for CO_2 Selective Adsorption. *Nat. Commun*. **2013**, *4*, 204-212.
54. Demessence, A.; D'Alessandro, D. M.; Foo, M. L.; Long, J. R. Strong CO_2 Binding in a Water-Stable, Triazolate Bridged Metal−Organic Framework Functionalized with Ethylenediamine. *J. Am. Chem. Soc*. **2009**, *131*, 8784-8786.
55. Alawisi, H.; Li, B.; He, Y.; Arman, H. D.; Asiri, A. M.; Wang, H.; Chen, B. A Microporous Metal–Organic Framework Constructed from a New Tetracarboxylic Acid for Selective Gas Separation. *Cryst. Growth Des*. **2014**, *14*, 2522-2526.
56. Rada, Z. H.; Abid, H. R.; Shang, J.; He, Y.; Webley, P.; Liu, S.; Sun, H.; Wang, S. Effects of Amino Functionality on Uptake of CO_2, CH_4 and Selectivity of CO_2/CH_4 on Titanium based MOFs. *Fuel* **2015**, *160*, 318-327.
57. Chen, K.-J.; Madden, D. G.; Pham, T.; Forrest, K. A.; Kumar, A.; Yang, Q.-Y.; Xue, W.; Space, B.; Perry IV, J. J.; Zhang, J.-P.; Chen, X.-M.; Zaworotko, M. J. Tuning Pore Size in Square-Lattice Coordination Networks for Size-Selective Sieving of CO_2. *Angew. Chem. Int. Ed.* **2016**, *55*, 10268–10272.
58. Wen, H. -M.; Liao, C.; Li, L.; Alsalme, A.; Alothman, Z.; Krishna, R.; Wu, H.; Zhou, W.; Hu, J.; Chen, B. A Metal–organic Framework with Suitable Pore Size and Dual Functionalities for Highly Efficient Post-combustion CO_2 Capture. *J. Mater. Chem. A* **2019**, *7*, 3128–3134.
59. Wang, B.; Cote, A. P.; Furukawa, H.; O'Keeffe, M.; Yaghi, O. M. Colossal Cages in Zeolitic Imidazolate Frameworks as Selective Carbon Dioxide Reservoirs. *Nature* **2008**, *453*, 207-211.
60. Pal, A.; Chand, S.; Madden, D. G.; Franz, D.; Ritter, L.; Johnson, A.; Space, B.; Curtin, T.; Das, M. C. A Microporous Co-MOF for Highly Selective CO_2 Sorption in High Loadings Involving Aryl C−H···O=C=O Interactions: Combined Simulation and Breakthrough Studies. *Inorg. Chem.* **2019**, *58*, 11553-11560.
61. Ye, Y.; Zhang, H.; Chen, L.; Chen, S.; Lin, Q.; Wei, F.; Zhang, Z.; Xiang, S. Metal–Organic Framework with Rich Accessible Nitrogen Sites for Highly Efficient CO_2 Capture and Separation. *Inorg. Chem.* **2019**, *58*, 7754-7759.
62. Lu, Z.; Meng, F.; Du, L.; Jiang, W.; Cao, H.; Duan, J.; Huang, H.; He, H. A Free Tetrazolyl Decorated Metal−Organic Framework Exhibiting High and Selective CO_2 Adsorption. *Inorg. Chem.* **2018**, *57*, 14018−14022.
63. Jiang, J.; Lu, Z.; Zhang, M.; Duan, J.; Zhang, W.; Pan, Y.; Bai, J. Higher Symmetry Multinuclear Clusters of Metal−Organic Frameworks for Highly Selective CO_2 Capture. *J. Am. Chem. Soc.* **2018**, *140*, 17825−17829.
64. Wang, Y.; Cao, H.; Zheng, B.; Zhou, R.; Duan, J. Solvent- and pH-Dependent Formation of Four Zinc Porous Coordination Polymers: Framework Isomerism and Gas Separation. *Cryst. Growth Des.* **2018**, *18*, 7674−7682.
65. Song, X.; Zhang, M.; Duan, J.; Bai, J. Constructing and Finely Tuning the CO_2 Traps of Stable and Various-pore-containing MOFs Towards Highly Selective CO_2 capture. *Chem. Commun.* **2019**, *55*, 3477-3480.
66. Lee, C. Y.; Bae, Y. –S.; Jeong, N. C.; Farha, O. K.; Sarjeant, A. A.; Stern, C. L.; Nickias, P.; Snurr, R. Q.; Hupp, J. T.; Nguyen, S. T. Kinetic Separation of Propene and Propane in Metal-Organic Frameworks: Controlling Diffusion Rates in Plate-Shaped Crystals via

Tuning of Pore Apertures and Crystallite Aspect Ratios. *J. Am. Chem. Soc.* **2011**, *133*, 5228–5231.

67. Li, K.; Olson, D. H.; Seidel, J.; Emge, T. J.; Gong, H.; Zeng, H.; Li, J. Zeolitic Imidazolate Frameworks for Kinetic Separation of Propane and Propene. *J. Am. Chem. Soc.* **2009**, *131*, 10368–10369.
68. Liu, J.; Wang, Y.; Benin, A. I.; Jakubczak, P.; Willis, R. R.; LeVan, M. D. CO_2/H_2O Adsorption Equilibrium and Rates on Metal-Organic Frameworks: HKUST-1 and Ni/DOBDC. *Langmuir* **2010**, *26*, 14301–14307.
69. Kizzie, A. C.; Wong-Foy, A. G.; Matzger, A. J. Effect of Humidity on the Performance of Microporous Coordination Polymers as Adsorbents for CO_2 Capture. *Langmuir* **2011**, *27*, 6368–6373.

Graphical Abstract